*First publ. in: Physica A: Statistical Mechanics and its Applications 232 (1996), 1-2, pp. 40-50*

# Dynamics of domains in diluted antiferromagnets

U. Nowak *, J. Esser, K.D. Usadel

*Theoretische Tieftemperaturphysik, Gerhard-Mercator-Universität-Duisburg, 47048 Duisburg, Germany*

Received 22 March 1996

**Abstract**

We investigate the dynamics of two-dimensional site-diluted Ising antiferromagnets. In an external magnetic field these highly disordered magnetic systems have a domain structure which consists of fractal domains with sizes on a broad range of length scales. We focus on the dynamics of these systems during the relaxation from a long-range ordered initial state to the disordered fractal-domain state after applying an external magnetic field. The equilibrium state with applied field consists of fractal domains with a size distribution which follows a power law with an exponential cutoff. The dynamics of the system can be understood as a growth process of this fractal-domain state in such a way that the equilibrium distribution of domains develops during time. Following these ideas quantitatively we derive a simple description of the time dependence of the order parameter. The agreement with simulations is excellent.

*PACS:* 75.10.Hk, 75.50.Lk, 75.40.Gb
*Keywords*: Ising-models; Random magnets; Dynamics

## 1. Introduction

One starting point for the theoretical investigation of the behavior of random magnets and related systems is to consider the system as consisting of finite ordered regions, called clusters, domains or droplets. In this article we want to consider the case of highly disordered systems where the magnetic structure consists of fractal domains with domain sizes on a broad range of length scales and we will derive a simple theoretical description based on scaling ideas. Nearly all of the assumptions we make and scaling relations we use will be proven in detail by exact ground state calculations as well as by Monte Carlo simulations.

The system we consider is the 2D diluted Ising antiferromagnet in an external magnetic field (DAFF) which can be used to study typical behavior of strongly disordered

* Corresponding author. e-mail: uli@thp.uni-duisburg.de.

systems as there are metastability, slow dynamics, and domain structures [1]. Related systems like random-field systems which are thought to be in the same universality class like the DAFF [2] or spin glasses may behave similarly.

The Hamiltonian of the DAFF in units of the next-neighbor coupling constant $J$ reads

$$H = \sum_{\langle i,j \rangle} \varepsilon_i \varepsilon_j \sigma_i \sigma_j - \sum_{i=1}^{N} B \varepsilon_i \sigma_i \tag{1}$$

where $\sigma_i = \pm 1$ denote Ising-spins and $\varepsilon_i = 0, 1$ a quenched disorder.

The phase diagram of the 2D DAFF consists of an antiferromagnetic low temperature phase for magnetic field $B = 0$ and a disordered phase for all finite values of $B$. In contrast, in three dimensions there exists a long-range ordered phase also for small magnetic fields [3]. For higher fields and low temperatures the DAFF develops a disordered domain state, both in two and three dimensions. This domain state has many of the characteristics of a spin glass, as for instance a remanent magnetization and an irreversibility line scaling like the deAlmeida–Thouless line [4]. For large disorder the domains have been shown to have a fractal structure [5] with a broad distribution of domain sizes and with scaling laws strongly deviating from the usual Imry–Ma assumptions [6] which are thought to be correct in the limit of small disorder.

We focus on the dynamics of the 2D DAFF during relaxation from a long-range ordered system to the fractal-domain state and describe this process in terms of a certain growth process dominated by thermal activation. In order to prove this approach in detail we use two numerical techniques to investigate 2D systems with a size of $700 \times 700$ on a square lattice and a dilution of 30%.

In Monte Carlo (MC) simulations [7] we use the standard heat-bath algorithm. Due to the slow dynamics of the DAFF at low temperatures it is extremely difficult to investigate equilibrium properties using MC techniques. Therefore, additionally we calculate the highly non-trivial ground states of the DAFF exactly using methods known from graph theory [8]. The Ising system is mapped on a graph and the maximum flow through the graph is determined by the Ford–Fulkerson algorithm [9]. The combination of these two methods, MC simulation and exact ground state (EGS) calculation, allows a precise investigation of both dynamics and equilibrium properties at finite temperatures and at $T = 0$.

## 2. Ground state properties

The geometrical properties of domains in random magnets are important as a starting point for theoretical considerations as well as for the interpretation of experimental results. In order to investigate the structure of the domain state of a simulated DAFF we perform a cluster analysis with a suitable adjusted Hoshen–Kopelman-type algorithm [10]. This algorithm pieces the system into domains. A domain is uniquely defined as a group of spins which are connected and antiferromagnetically ordered. In

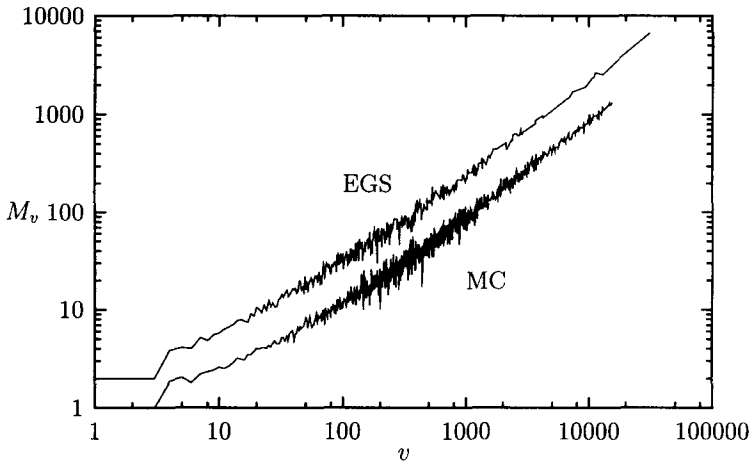


Fig. 1. Magnetisation $M_v$ versus volume $v$ of the domains of the fractal-domain state of the 2D DAFF. Comparison of MC simulations (average over 50 systems of size 199 × 198) and EGS calculations (average over 10 systems of size 400 × 400). The latter curve is shifted by a factor 2. $B = 1.5$. All quantities are dimensionless.

Table 1
Scaling relations for the DAFF

| | | | | | |
|---|---|---|---|---|---|
| $D = 3$ | $v \sim R^{2.0}$ | $F \sim v$ | $M_v \sim v$ | $E_w \sim F$ | – |
| $D = 2$ | $v \sim R^{1.56}$ | $F \sim v$ | $M_v \sim v$ | $E_w \sim F$ | $n \sim v^{-1.5} \exp(-v/v_0)$ |

this way, it is possible to compute directly the volume $v$ (number of spins), surface $F$ (number of unsatisfied bonds) and radius $R$ (root of the mean squared distance of spins) of the domains formed (note that in two dimensions $v$ is the area and $F$ the border of the domains). Also one can compute the corresponding energy-relevant quantities, like domain wall energy $E_w$ (number of broken bonds) and volume-magnetization $M_v$ for all domains.

The fractal properties of the domain state calculated by MC simulation have been reported earlier [4, 5]. For high disorder we discovered a fractal and interpenetrating structure of the domains fulfilling scaling relations which are strongly deviating from the assumptions of the Imry–Ma argument [6]. These earlier findings are also correct for the EGS reported here for the first time for the 2D DAFF. Fig. 1 shows the volume-magnetization $M_v(v)$, i.e. the mean volume-magnetization $M_v$ of domains with size $v$. The scaling behavior is identical with that for the domains calculated by MC simulation – which are inevitably out of equilibrium. For 3D systems this has been shown earlier [8]. As Fig. 1 shows the scaling relation $M_v(v) \sim v^{d_m}$ holds for large enough $v$. All scaling relations of the DAFF obtained so far are summarized in Table 1.

An important quantity is the distribution of domain sizes found in the domain state of the 2D DAFF. In the next section we will use this distribution function for a description of the dynamics of the DAFF. Fig. 2 shows the number of domains $N$ for

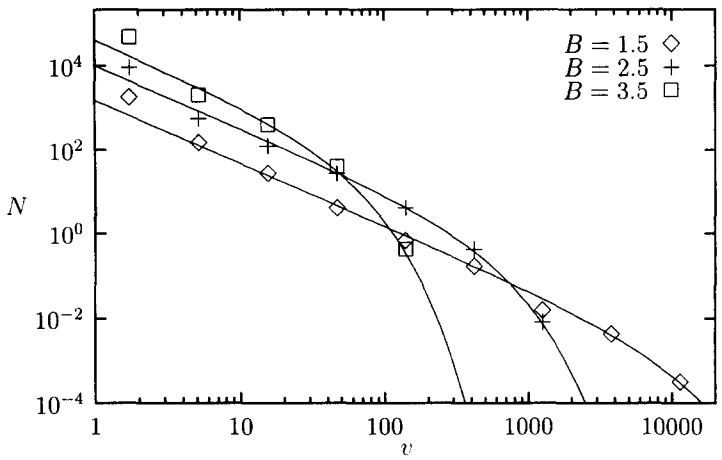


Fig. 2. $N$ versus $v$ from EGS calculations for different fields $B$. Apart from the average over 10 systems of size $400 \times 400$ the data are additionally averaged in such a way that they show the relative number of domains having a volume within a certain interval $\Delta v$. The lines are fits to Eq. (2).

a given volume $v$ from EGS calculations. Since the number of domains is a strongly fluctuating quantity the data are averaged over intervals of volumes $\Delta v$. The width of these intervals is increased exponentially so that we have a constant distance between points on a logarithmic scale. The data are well described by a power-law with an exponential cutoff,

$$N(v) = N_0 v^{-d_n} e^{-v/v_0}. \tag{2}$$

The lines in Fig. 2 are fits to Eq. (2). The cutoff parameter $v_0$ is field dependent. Although the fractal dimensions of the domains of the DAFF are the same as those known from percolation [11] the exponent $d_n \approx 1.5$ is between that for critical percolation clusters ($d_n = 187/91$) and that for lattice animals ($d_n = 1$). A possible small field dependence of this exponent cannot be ruled out. Also, the isolated clusters from the percolation problem lead to the systematic deviation from the power law in Fig. 2 for very small volumes, $v < 5$. Since there is no infinite domain in the system we do not consider a stretched exponential cutoff in Eq. (2) (the latter is known from the percolation problem if there is an infinite cluster). Summed up, the domains of the DAFF have the structure of the lattice animals of the percolation problem but with a different exponent $d_n$ in the distribution function.

The distribution function Eq. (2) is a central quantity of a domain state since other quantities follow from this distribution. E.g. the order parameter $M_s$ per spin can be rewritten as the sum over all domain sizes $v$ of the corresponding order parameters times the number of domains of that size:

$$M_s = \int_1^\infty \mathrm{d}v\, n(v) M_s(v), \tag{3}$$

where $n(v)$ is the distribution of domain sizes normalized in such a way that $M_s$ is the staggered magnetization per spin.

In the next section we will use the equations above as the starting point for a description of the dynamics of the DAFF.

## 3. Dynamics

We focus on the dynamics of the two-dimensional DAFF. As was discussed in the preceeding section the equilibrium state of the system in a finite field consists of antiferromagnetically ordered domains with a size distribution following Eq. (2). When we start the dynamics with an antiferromagnetically long-range ordered system how does the system evolve into this fractal-domain state?

Fig. 3 shows a ground state configuration from EGS calculations (bottom) and two configurations of the same system (i.e. with same configuration of vacancies) during the MC simulation. For these pictures we restrict ourselves to a small system of size $100 \times 100$. We start the simulation with a long-range ordered state (white) and switch on a field $B = 1.5$ and a finite temperature $T = 0.4$.

The ground state of our system is essentially unique (see Ref. [8] for details). It is a domain pattern that is stored in the system through the vacancy configuration and the field and it is the equilibrium state of the system. How is this domain pattern reconstructed in our Monte Carlo simulation?

As Fig. 3 suggests, during the relaxation from the long-range ordered initial state to the fractal-domain state, the dynamics of the system can be understood as a kind of growth process. For shorter times only small domains arise. Interestingly, these small domains are located at those places where later the larger domains will be. At later times, *also* larger domains occur and the size of the largest domains increases in time. The pictures lead us to the following description of the growth process: the equilibrium distribution of domains develops starting with the smaller domains and increasing the maximum domain size in time.

In order to investigate this process quantitatively we simulate the size distribution of domains during the relaxation process. Fig. 4 shows the equilibrium distribution from EGS calculations and distributions of domains that are reversed after five different times of MC simulation. For a given time $t$ the system has obviously a distribution that is equal to the equilibrium distribution $n(v)$ corresponding to Eq. (2) up to the largest domain size $v_m(t)$ that has developed at that time by thermal activation. Note that this time dependent cutoff in the distribution function is very abrupt since Fig. 4 shows data over a range of eight decades. These considerations lead to the following description of the time development of the order parameter $M_s$. We start with a long-range ordered system, i.e. $M_s(t = 0) = M_{si} \approx 1$.[1] After switching on the field the

[1] Note that $\lim_{t \to 0} M_s < 1$ since due to the dilution there are spins or clusters of spins that are not or only weakly connected to the infinite cluster. These clusters may have finite magnetizations which follow the external field immediately since there are no relevant energy barriers.

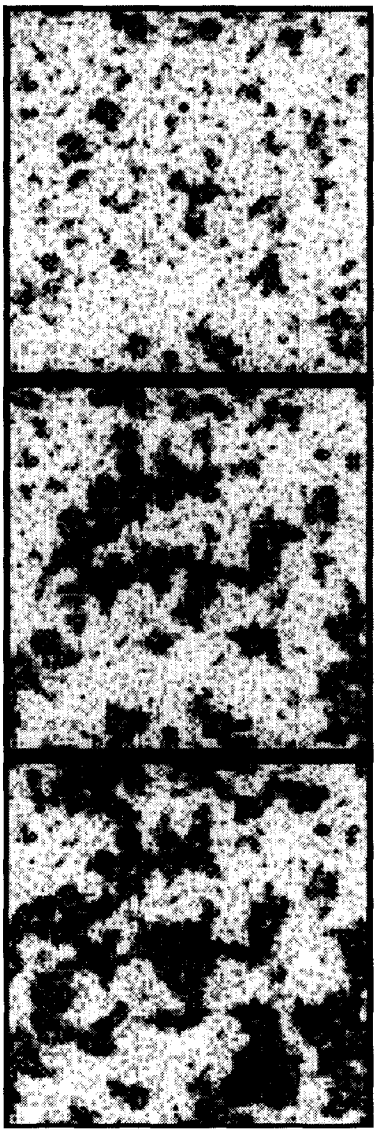

Fig. 3. EGS of a $100 \times 100$ system (bottom) and two configurations of the system during the MC simulation of the relaxation process after roughly 500 MCS (top) and 130 000 MCS (center). $T = 0.4$, $B = 1.5$. The two antiferromagnetic phases are represented in black and white, the vacancies are grey.

staggered magnetization decreases to $M_s(t \to \infty) = M_{s\infty} \approx 0$ (except of finite-size effects) due to the growth of domains of the other phase:

$$M_s(t) = M_{si} + 2 \int_1^{v_m(t)} \mathrm{d}v\, n(v) M_s(v). \tag{4}$$

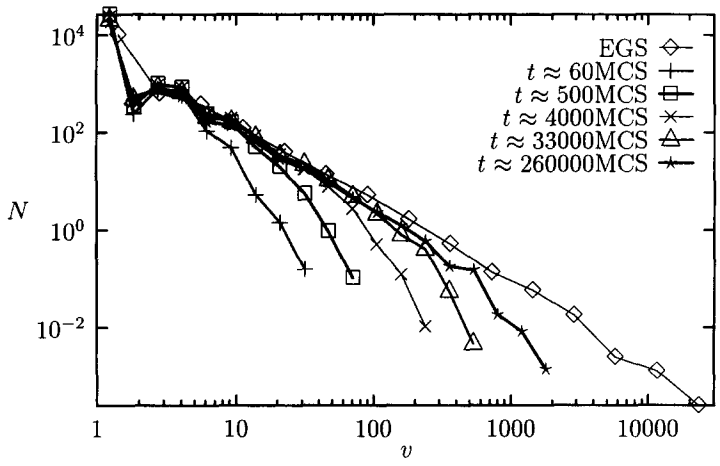


Fig. 4. $N$ versus $v$ during MC simulation of the relaxation process and for the EGS of the same $700 \times 700$ system (see Fig. 2 for explanation). $T = 0.4$, $B = 1.5$.

Since a domain is defined as a group of spins which are antiferromagnetically ordered it is per definition $M_s(v) = -v$ for the reversed domains so that

$$\begin{aligned} M_s(t) &= M_{si} - 2\int_1^{v_m(t)} \mathrm{d}v\, n_0 v^{1-d_n} e^{-v/v_0} \\ &= M_{s\infty} + 2n_0 \int_{v_m(t)}^{\infty} \mathrm{d}v\, v^{1-d_n} e^{-v/v_0} \\ &\equiv M_{s\infty} + \gamma(v_m(t)) \end{aligned} \tag{5}$$

where the last line defines the function $\gamma(v_m(t))$. $n_0$ is defined by the normalization condition

$$2\int_1^{\infty} \mathrm{d}v\, n_0 v^{1-d_n} e^{-v/v_0} + M_{s\infty} = M_{si}. \tag{6}$$

According to the preceeding section the exponent is $d_n = 1.5$ and the field dependent cutoff parameter can be obtained from EGS calculations. Thus $\gamma(v_m(t))$ is well defined without any unknown parameters. Since the integration cannot be done exactly it will be calculated numerically. Furthermore, the integral $\gamma(v_m(t))$ is related to the so-called incomplete Gamma function

$$\Gamma(\alpha, x) \equiv \int_0^x \mathrm{d}y\, y^{\alpha-1} e^{-y} \tag{7}$$

the properties of which we will discuss later.

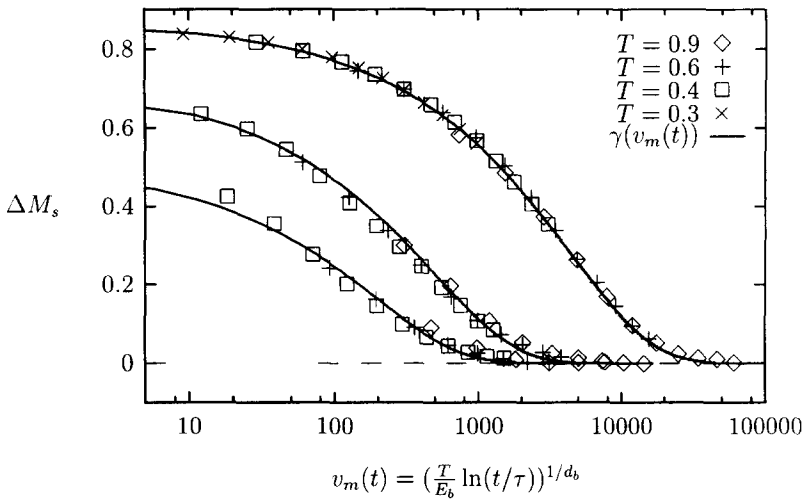


Fig. 5. Scaling plot for the order parameter $\Delta M_s = M_s(t) - M_{s\infty}$. Data are shown for three different fields $B = 1.5, 2.0, 2.5$ (from above); and four temperatures in field $B = 1.5$ and three temperatures in field $B = 2.0, 2.5$. The time ranges from 95 to 200 000 MCS. The solid lines are the theoretical curves following Eq. (5) with $v_0 = 9000$ ($B = 1.5$), 1000 ($B = 2.0$), 400 ($B = 2.5$).

It is highly plausible that the largest existing domain size $v_m(t)$ for a time $t$ is connected to a thermal activation energy $\Delta E(t) = T \ln(t/\tau)$ according to

$$\Delta E(t) = E_b v_m^{d_b}(t) \tag{8}$$

where $d_b$ is an exponent connecting the size of domains with a free-energy barrier $\Delta E$ which has to be overcome during the buildup of a domain of size $v_m$. This assumption of thermal activation gives the time dependence of $M_s$ in Eq. (5).

In order to prove the validity of our approach we use MC simulation data for the decay of the order parameter. In Fig. 5 we show data for three different values of the magnetic field $B = 1.5, 2.0, 2.5$. The way we evaluate the simulation data is the following:

(i) First of all, due to the equations above data for the relaxation for different temperatures should collapse in a scaling plot $M_s$ versus any function $f(T \ln(t/\tau))$ where $\tau$ should be a microscopic time scale for the growth of the smallest domains. In Fig. 5 the data for four temperatures in field $B = 1.5$ and for three temperatures in field $B = 2.0, 2.5$ with a time window ranging from 95 to 200 000 MCS are seen to collapse very well using $\tau = 3$ MCS. We do not consider time scales much shorter than 100 MCS because then thermal fluctuations cannot be neglected.

(ii) Finding the correct barrier exponent $d_b$ and the prefactor $E_b$ we can determine $v_m(t) = ((T/E_b) \ln(t/\tau))^{1/d_b}$ and following Eq. (5) the data for $M_s(t) - M_{s\infty}$ should be described by $\gamma(v_m(t))$. As Fig. 5 shows this works perfectly for the complete range of the scaling variable $v$ and for three different fields using $d_b = 0.25$. Note that the reason

for the field dependence of $\gamma(v_m(t))$ is the field dependence of the cutoff parameter $v_0$ which has been obtained by EGS calculations (see Fig. 2).

The data for the two higher fields are less accurate since in this case the dynamics is faster and has a shorter observation time. Additionally for the higher fields we restricted ourselves to smaller lattices ($400 \times 400$ instead of $700 \times 700$ for $B = 1.5$) since the EGS calculations are very time consuming. However, no field dependence of the barrier exponent can be seen. The prefactor $E_b$ is slightly field dependent ($E_b = 0.60$ ($B = 1.5$), $0.74$ ($B = 2.0$), $0.67$ ($B = 2.5$)). Note that since the barrier exponent is very small we are close to the case $\Delta E(t) \sim \ln(v_m(t))$ which is the limit $d_b \to 0$ in Eq. (8).

Of course, other quantities can be described in a similar manner. E.g. for large enough volumes $v$ (see Fig. 1) the magnetization $M$ can be written correspondingly as

$$M(t) = M_i + 2 \int_1^{v_m(t)} \mathrm{d}v \, n_0 M_0 v^{d_m - d_n} e^{-v/v_0}. \tag{9}$$

The magnetization $M$ is a quantity that can be measured experimentally. Its precise behavior has to be obtained from a numerical integration of Eq. (9). Two for the description of experimental data relevant limits can however be obtained asymptotically as limits of the Gamma function.

The first limit is that of short times and small temperatures where the exponential cutoff is irrelevant which means $((T/E_b)\ln(t/\tau))^{1/d_b} = v \ll v_0$ and consequently $e^{-v/v_0} \approx 1$ resulting in

$$\begin{aligned} M(t) &\approx M_i + 2n_0 M_0 (v(t))^{d_m - d_n + 1} \\ &= M_i + 2n_0 M_0 \left( \frac{T}{E_b} \ln(t/\tau) \right)^{(d_m - d_n + 1)/d_b} . \end{aligned} \tag{10}$$

This is a logarithmic law with a temperature-independent exponent obtained from the fractality and the distribution of the equilibrium domains and from the free-energy barriers that have to be overcome to build up these domains. Similar logarithmic laws are usually used to describe experimental data of the dynamics of the DAFF (for a review of the experimental work see [12]). Note that $M_i$ is not zero but has a small finite value for the same reason that has been explained earlier – see the discussion of $M_{si}$.

The second limit is that close to equilibrium, i.e. for long times and higher temperatures. Here we can use an asymptotic form of the Gamma function

$$\lim_{x \to \infty} \Gamma(\alpha, x) \sim x^{\alpha - 1} e^{-x}.$$

The restriction to the most relevant term, the $e$-function, results in

$$M(t) \sim \exp - \left( \frac{T}{E_b} \ln \left( \frac{t}{\tau} \right) \right)^{1/d_b/v_0} \tag{11}$$

$$\sim t^{-T/(E_b v_0)} \quad \text{for } d_b = 1. \tag{12}$$

The generalized power law Eq. (11) has been used to fit experimental data as well as data from MC simulations for the remanent magnetization of the 3D DAFF [13, 14]. For $d_b = 1$ it simplifies to a simple power law with the exponent proportional to the temperature. This law has also been discussed as a description of the remanent magnetization of the 3D DAFF [15] and it is typical for the decay of the remanent magnetization of spin glasses (see [16] for a review).

## 4. Conclusions

We derived a simple description for the dynamics of the 2D DAFF during the relaxation from long-range order to a fractal-domain state. The basic fundamentals of this description are the fractality and the distribution of the domains the domain state of the system consists of in the limit of high disorder. This is the main extension to earlier theories for the case of weak disorder based on scaling assumptions for domains which are compact and non-fractal. These domains have for a certain time scale a unique relevant length scale – the domain radius (see e.g. [6, 17] for scaling theories of random-field models and [17, 18] for a description of domain dynamics in terms of domain wall motion).

As a result of our approach which is based on measured quantities of the domain state the dynamics can be described with the assumption of thermal activation analytically and is given by an incomplete Gamma function. As one advantage this function connects naturally two for disordered systems often observed laws as limiting cases – the logarithmic law in the limit of short times and low temperatures and the (generalized) power law in the limit of late times and higher temperatures. Apart from that our approach illustrates that from the fact that a system has a distribution of domain sizes instead of one dominating size follows that the mean domain size of that distribution can grow following a power law (Eq. (12)) even if the largest domain in the system is built by thermal activation, i.e. within a logarithmic time scale (see e.g. [16] for a summary of this apparent contradiction in spin glasses).

The agreement with simulations is excellent. However, so far we are not aware of any direct experimental observation of this kind of dynamics in 2D DAFF although as mentioned above similar laws are often observed in the dynamics of disordered magnets and we assume that a similar description might also work for other strongly disordered systems like random-field systems or spin glasses.

## Acknowledgements

The authors wish to thank M. Staats for technical help. The work was supported by the Deutsche Forschungsgemeinschaft through Sonderforschungsbereich 166.

## References


[1] D.P. Belanger and A.P. Young, J. Magn. Magn. Mater. 100 (1991) 272.
[2] S. Fishman and A. Aharony, J. Phys. C 12 (1979) L729.
[3] J.Z. Imbrie, Phys. Rev. Lett. 53 (1984) 1747;
J. Bricmont and A. Kupiainen, Phys. Rev. Lett. 59 (1987) 1829.
[4] U. Nowak and K.D. Usadel, Phys. Rev. B 44 (1991) 7426.
[5] U. Nowak and K.D. Usadel, Phys. Rev. B 46 (1992) 8329.
[6] Y. Imry and S. Ma, Phys. Rev. Lett. 35 (1975) 1399.
[7] K. Binder and D.W. Heermann, Monte Carlo Simulations in Statistical Physics (Springer, Berlin, 1988)
[8] A. Hartmann and K.D. Usadel, Physica A 214 (1995) 141.
[9] M.N.S. Swamy and K. Thulasiraman, Graphs, Networks, and Algorithms (Wiley, New York, 1981);
J.P. Picard and H.D. Ratliff, Networks 5 (1975) 357.
[10] J. Hoshen and R. Kopelman, Phys. Rev. B 14 (1976) 3428.
[11] D. Stauffer and A. Aharony, Introduction to Percolation Theory (Taylor and Francis, London, 1992);
G. Parisi and N. Sourlas, Phys. Rev. Lett. 46 (1981) 871.
[12] W. Kleemann, J. Mod. Phys. B 7 (1993) 2469.
[13] S.-J. Han, D.P. Belanger, W. Kleemann and U. Nowak, Phys. Rev. B 45 (1992) 9728.
[14] S.-J. Han and D.P. Belanger, Phys. Rev. B 46 (1992) 2926.
[15] U. Nowak und K.D. Usadel, Phys. Rev. B 43 (1991) 851.
[16] H. Rieger, in: Annual Reviews of Computational Physics II, ed. D. Stauffer (World Scientific, Singapore, 1995) p. 295; D. Chowdhury and B. Biswal, in: Annual Reviews of Computational Physics I, ed. D. Stauffer (World Scientific, Singapore, 1994) p. 55.
[17] J. Villain, Phys. Rev. Lett. 52 (1984) 1543.
[18] T. Nattermann and I. Vilfan, Phys. Rev. Lett. 61 (1988) 223.